

Supplementary Materials for “Personalized Biopsies in Prostate Cancer Active Surveillance”

Anirudh Tomer, MSc^{a,*}, Dimitris Rizopoulos, PhD^a, Daan Nieboer, MSc^b,
Monique J. Roobol, PhD^c, Au Thor^d, Aut Hor^d, Auth Or^d

^a*Department of Biostatistics, Erasmus University Medical Center, Rotterdam, the Netherlands*

^b*Department of Public Health, Erasmus University Medical Center, Rotterdam, the Netherlands*

^c*Department of Urology, Erasmus University Medical Center, Rotterdam, the Netherlands*

^d*Department of xxxx, xxxx University Medical Center, City, Country*

1 Appendix A. A Joint Model for the Longitudinal PSA, and Time 2 to Gleason ≥ 7

3 Appendix A.1. Study Cohort

4 Prostate Cancer International Active Surveillance (PRIAS) is an ongoing
5 prospective cohort study of men with low- and very-low risk PCa diagnoses [1].
6 More than 100 medical centers from 17 countries contribute in PRIAS,
7 using a common study protocol (www.prias-project.org). We
8 used the data collected between December 2006 (beginning of PRIAS study)
9 and May 2019. The PSA was measured every three months until year two
10 of follow-up and every six months thereafter. Biopsy schedule was year one,
11 four, seven, and ten, and additional yearly biopsies when PSA doubling time
12 is between zero and ten years. The primary event of this work is Gleason ≥ 7
13 (GS7). It was observed in 1134 patients, but 2250 were provided treatment
14 (see Table 1). Treatment in absence of GS7 may have been advised on the
15 basis of PSA, number of biopsy cores with cancer, anxiety, or other reasons.

*Corresponding author (Anirudh Tomer): Erasmus MC, kamer flex Na-2823, PO Box 2040, 3000 CA Rotterdam, the Netherlands. Tel: +31 10 70 43393

Email addresses: a.tomer@erasmusmc.nl (Anirudh Tomer, MSc),
d.rizopoulos@erasmusmc.nl (Dimitris Rizopoulos, PhD), d.nieboer@erasmusmc.nl
(Daan Nieboer, MSc), m.roobol@erasmusmc.nl (Monique J. Roobol, PhD)

16 We focused only on GS7 because of its strong association with cancer-related
 17 outcomes. Due to the periodical nature of biopsies, the time of GS7 was only
 18 known as a time interval in which it occurred.

Table 1: **Patient characteristics for the PRIAS dataset.** The primary event of interest is Gleason ≥ 7 . IQR: interquartile range, PSA: prostate-specific antigen.

Characteristic	Value
Total patients	7813
Gleason ≥ 7 (primary event)	1134
Treatment	2250
Watchful waiting	334
Loss to follow-up	250
Death (unrelated to prostate cancer)	95
Death (related to prostate cancer)	2
Median age at diagnosis (years)	61 (IQR: 66–71)
Median follow-up period per patient (years)	1.8 (IQR: 0.9–3.99)
Total PSA measurements	65798
Median number of PSA measurements per patient	6 (IQR: 4–12)
Median PSA value (ng/mL)	5.7 (IQR: 4.1–7.7)
Total biopsies	15563
Median number of biopsies per patient	2 (IQR: 1–3)

19 Appendix A.2. Model Definition

20 Let T_i^* denote the true time of GS7 for the i -th patient included in PRIAS.
 21 Since biopsies are conducted periodically, T_i^* is observed with interval cen-
 22 soring $l_i < T_i^* \leq r_i$. When GS7 is observed for the patient at his latest biopsy
 23 time r_i , then l_i denotes the time of the second latest biopsy. Otherwise, l_i
 24 denotes the time of the latest biopsy and $r_i = \infty$. Let \mathbf{y}_i denote his ob-
 25 served PSA longitudinal measurements. The observed data of all n patients
 26 is denoted by $\mathcal{D}_n = \{l_i, r_i, \mathbf{y}_i; i = 1, \dots, n\}$.

In our joint model, the patient-specific PSA measurements over time are modeled using a linear mixed effects sub-model. It is given by (see Panel A, Figure 1):

$$\log_2 \{y_i(t) + 1\} = m_i(t) + \varepsilon_i(t),$$

$$m_i(t) = \beta_0 + b_{0i} + \sum_{k=1}^4 (\beta_k + b_{ki}) B_k \left(\frac{t-2}{2}, \frac{\mathcal{K}-2}{2} \right) + \beta_5 \text{age}_i, \quad (1)$$

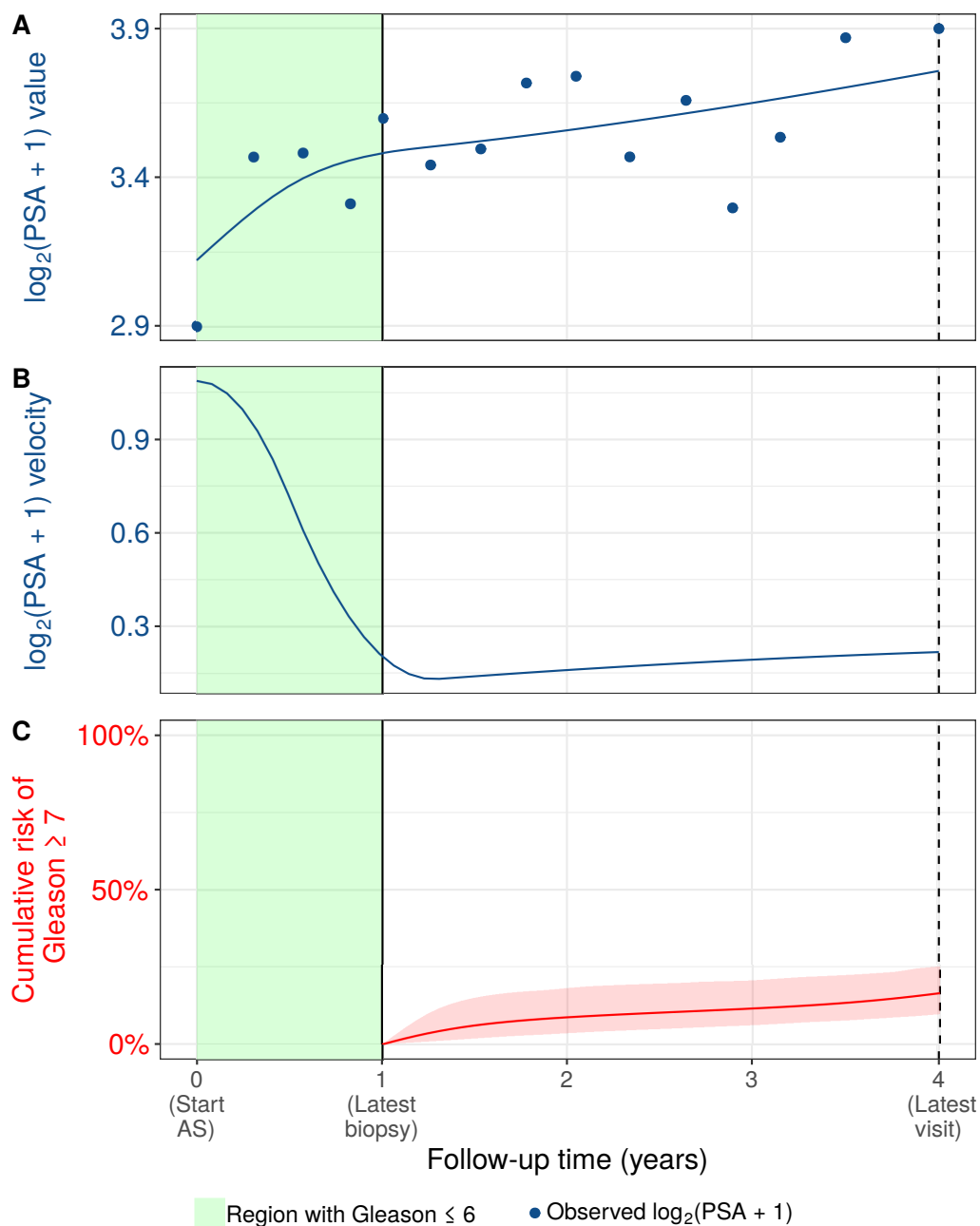


Figure 1: **Illustration of the joint model fitted to the PRIAS dataset.** **Panel A:** shows the observed and fitted $\log_2(\text{PSA} + 1)$ measurements (Equation 1). **Panel B:** shows the estimated $\log_2(\text{PSA} + 1)$ velocity over time, mathematically derived from Equation (1). The cumulative risk of Gleason ≥ 7 (Equation 2) shown in **Panel C**, depends on the fitted $\log_2(\text{PSA} + 1)$ value and velocity, and the time of the latest biopsy (year 1 in this case).

where, $m_i(t)$ denotes the measurement error free value of $\log_2(\text{PSA} + 1)$ transformed [2, 3] measurements at time t . We model it non-linearly over time using B-splines [4]. To this end, our B-spline basis function $B_k\{(t - 2)/2, (\mathcal{K} - 2)/2\}$ has 3 internal knots at $\mathcal{K} = \{0.5, 1.3, 3\}$ years, which are the three quartiles of the observed follow-up times. The boundary knots of the spline are at 0 and 6.3 years (95-th percentile of the observed follow-up times). We mean centered (mean 2 years) and standardized (standard deviation 2 years) the follow-up time t and the knots of the B-spline \mathcal{K} during parameter estimation for better convergence. The fixed effect parameters are denoted by $\{\beta_0, \dots, \beta_5\}$, and $\{b_{0i}, \dots, b_{4i}\}$ are the patient specific random effects. The random effects follow a multivariate normal distribution with mean zero and variance-covariance matrix \mathbf{D} . The error $\varepsilon_i(t)$ is assumed to be t-distributed with three degrees of freedom (see Appendix B.1) and scale σ , and is independent of the random effects.

To model the impact of PSA measurements on the risk of GS7, our joint model uses a relative risk sub-model. More specifically, the hazard of GS7 denoted as $h_i(t)$, and the cumulative risk of GS7 denoted as $R_i(t)$, at a time t are (see Panel C, Figure 1):

$$\begin{aligned} h_i(t) &= h_0(t) \exp \left(\gamma \text{age}_i + \alpha_1 m_i(t) + \alpha_2 \frac{\partial m_i(t)}{\partial t} \right), \\ R_i(t) &= \exp \left\{ - \int_0^t h_i(s) ds \right\}, \end{aligned} \quad (2)$$

where, γ is the parameter for the effect of age. The impact of PSA on the hazard of GS7 is modeled in two ways, namely the impact of the error free underlying PSA value $m_i(t)$ (see Panel A, Figure 1), and the impact of the underlying PSA velocity $\partial m_i(t)/\partial t$ (see Panel B, Figure 1). The corresponding parameters are α_1 and α_2 , respectively. Lastly, $h_0(t)$ is the baseline hazard at time t , and is modeled flexibly using P-splines [5]. More specifically:

$$\log h_0(t) = \gamma_{h_0,0} + \sum_{q=1}^Q \gamma_{h_0,q} B_q(t, \mathbf{v}),$$

where $B_q(t, \mathbf{v})$ denotes the q -th basis function of a B-spline with knots $\mathbf{v} = v_1, \dots, v_Q$ and vector of spline coefficients γ_{h_0} . To avoid choosing the number and position of knots in the spline, a relatively high number of knots (e.g., 15 to 20) are chosen and the corresponding B-spline regression coefficients γ_{h_0} are penalized using a differences penalty [5].

46 *Appendix A.3. Parameter Estimation*

We estimate the parameters of the joint model using Markov chain Monte Carlo (MCMC) methods under the Bayesian framework. Let $\boldsymbol{\theta}$ denote the vector of all of the parameters of the joint model. The joint model postulates that given the random effects, the time of GS7, and the PSA measurements taken over time are all mutually independent. Under this assumption the posterior distribution of the parameters is given by:

$$\begin{aligned} p(\boldsymbol{\theta}, \mathbf{b} \mid \mathcal{D}_n) &\propto \prod_{i=1}^n p(l_i, r_i, \mathbf{y}_i \mid \mathbf{b}_i, \boldsymbol{\theta}) p(\mathbf{b}_i \mid \boldsymbol{\theta}) p(\boldsymbol{\theta}) \\ &\propto \prod_{i=1}^n p(l_i, r_i \mid \mathbf{b}_i, \boldsymbol{\theta}) p(\mathbf{y}_i \mid \mathbf{b}_i, \boldsymbol{\theta}) p(\mathbf{b}_i \mid \boldsymbol{\theta}) p(\boldsymbol{\theta}), \\ p(\mathbf{b}_i \mid \boldsymbol{\theta}) &= \frac{1}{\sqrt{(2\pi)^q \det(\mathbf{D})}} \exp(\mathbf{b}_i^T \mathbf{D}^{-1} \mathbf{b}_i), \end{aligned}$$

where, the likelihood contribution of the PSA outcome, conditional on the random effects is:

$$p(\mathbf{y}_i \mid \mathbf{b}_i, \boldsymbol{\theta}) = \frac{1}{(\sqrt{2\pi}\sigma^2)^{n_i}} \exp\left(-\frac{\|\mathbf{y}_i - \mathbf{m}_i\|^2}{\sigma^2}\right),$$

The likelihood contribution of the time of GS7 outcome is given by:

$$p(l_i, r_i \mid \mathbf{b}_i, \boldsymbol{\theta}) = \exp\left\{-\int_0^{l_i} h_i(s) ds\right\} - \exp\left\{-\int_0^{r_i} h_i(s) ds\right\}. \quad (3)$$

47 The integral in (3) does not have a closed-form solution, and therefore we
48 use a 15-point Gauss-Kronrod quadrature rule to approximate it.

49 We use independent normal priors with zero mean and variance 100 for
50 the fixed effects $\{\beta_0, \dots, \beta_5\}$, and inverse Gamma prior with shape and rate
51 both equal to 0.01 for the parameter σ^2 . For the variance-covariance matrix
52 \mathbf{D} of the random effects we take inverse Wishart prior with an identity scale
53 matrix and degrees of freedom equal to 5 (number of random effects). For
54 the relative risk model's parameter γ and the association parameters α_1, α_2 ,
55 we use independent normal priors with zero mean and variance 100.

56 *Appendix A.4. Parameter Estimates*

57 The joint model was fitted using the R package **JMbayes** [6]. This pack-
58 age utilizes the Bayesian methodology to estimate model parameters. The

corresponding posterior parameter estimates are shown in Table 3 (longitudinal sub-model for PSA outcome) and Table 4 (relative risk sub-model). The parameter estimates for the variance-covariance matrix \mathbf{D} from the longitudinal sub-model for PSA are shown in the following Table 2:

Table 2: Estimated variance-covariance matrix \mathbf{D} of the random effects $\mathbf{b} = (b_0, b_1, b_2, b_3, b_4)$ (see Appendix A.2) from the joint model fitted to the PRIAS dataset. The variances of the random effects are highlighted along the diagonal of the variance-covariance matrix.

Random Effects	b_0	b_1	b_2	b_3	b_4
b_0	0.229	0.029	0.022	0.070	0.005
b_1	0.029	0.149	0.097	0.169	0.085
b_2	0.022	0.097	0.270	0.326	0.231
b_3	0.070	0.169	0.326	0.550	0.355
b_4	0.005	0.085	0.231	0.355	0.348

For the PSA mixed effects sub-model parameter estimates (see Equation 1), in Table 3 we can see that the age of the patient trivially affects the baseline $\log_2(\text{PSA} + 1)$ measurement. Since the longitudinal evolution of $\log_2(\text{PSA} + 1)$ measurements is modeled with non-linear terms, the interpretation of the coefficients corresponding to time is not straightforward. In lieu of the interpretation, in Figure 2 we present plots of observed versus fitted PSA profiles for nine randomly selected patients.

Table 3: Estimated mean and 95% credible interval for the parameters of the longitudinal sub-model (see Equation 1) for the PSA outcome.

Variable	Mean	Std. Dev	2.5%	97.5%	P
Intercept	2.124	0.054	2.024	2.236	<0.001
Age	0.009	0.001	0.007	0.010	<0.001
Spline: [0.0, 0.5] years	0.062	0.006	0.050	0.075	<0.001
Spline: [0.5, 1.3] years	0.194	0.011	0.175	0.214	<0.001
Spline: [1.3, 3.0] years	0.243	0.014	0.218	0.269	<0.001
Spline: [3.0, 6.3] years	0.382	0.014	0.356	0.408	<0.001
σ	0.139	0.001	0.137	0.140	

For the relative risk sub-model (see Equation 2), the parameter estimates in Table 4 show that $\log_2(\text{PSA} + 1)$ velocity and age of the patient were significantly associated with the hazard of GS7.

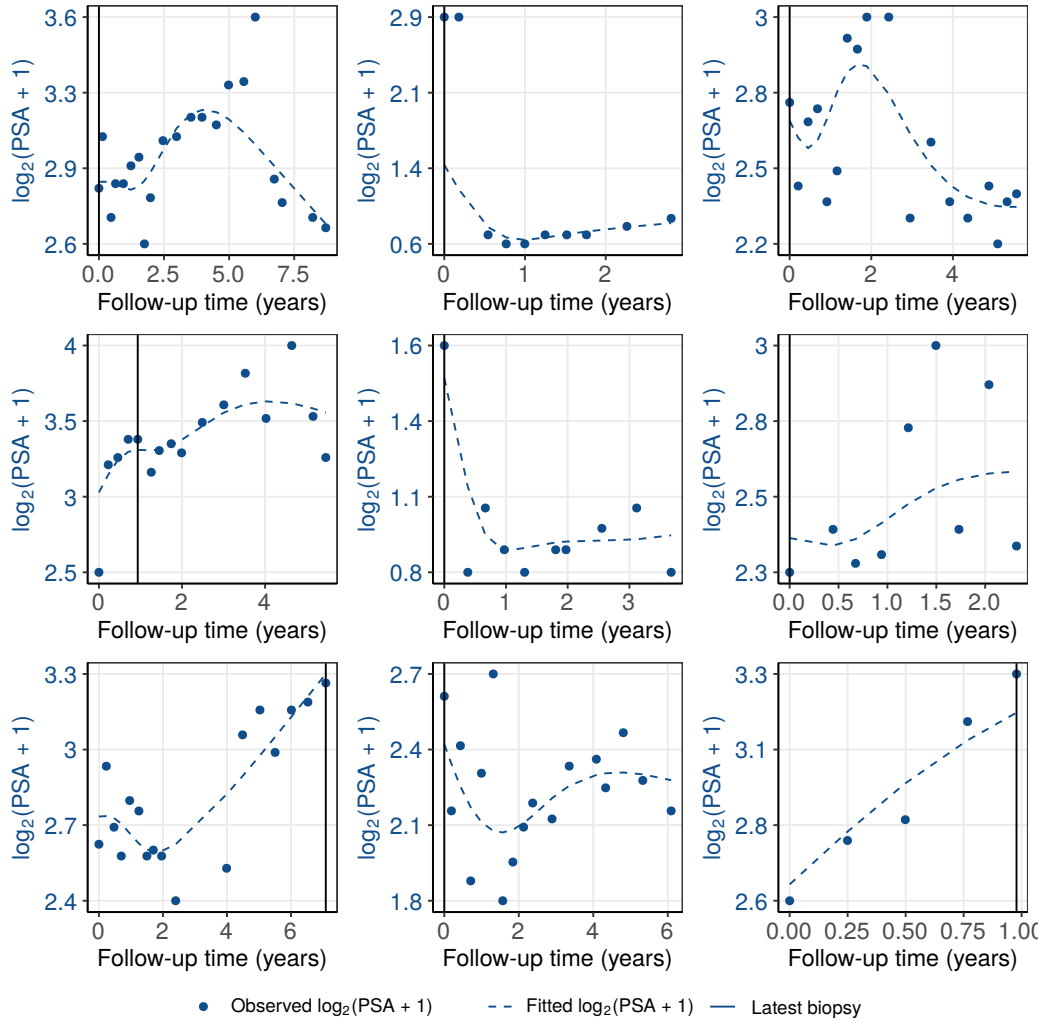


Figure 2: Fitted versus observed $\log_2(\text{PSA} + 1)$ profiles for nine randomly selected PRIAS patients. The fitted profiles utilize information from the observed PSA measurements, and time of the latest biopsy.

Table 4: Estimated mean and 95% credible interval for the parameters of the relative risk sub-model (see Equation 2) of the joint model fitted to the PRIAS dataset.

Variable	Mean	Std. Dev	2.5%	97.5%	P
Age	0.037	0.006	0.026	0.049	<0.001
Fitted $\log_2(\text{PSA} + 1)$ value	-0.013	0.078	-0.157	0.143	0.812
Fitted $\log_2(\text{PSA} + 1)$ velocity	2.297	0.303	1.670	2.789	<0.001

73 It is important to note that since age, and $\log_2(\text{PSA} + 1)$ value and ve-
74 locity are all measured on different scales, a comparison between the cor-
75 responding parameter estimates is not easy. To this end, in Table 5, we
76 present the hazard (of GS7) ratio, for an increase in the aforementioned vari-
77 ables from their first to the third quartile. For example, an increase in fitted
78 $\log_2(\text{PSA} + 1)$ velocity from -0.086 to 0.307 (fitted first and third quartiles)
79 corresponds to a hazard ratio of 2.466. The interpretation for the rest is
80 similar.

Table 5: Hazard (of GS7) ratio and 95% credible interval (CI), for an increase in the variables of relative risk sub-model, from their first quartile (Q_1) to their third quartile (Q_3). Except for age, quartiles for all other variables are based on their fitted values obtained from the joint model fitted to the PRIAS dataset.

Variable	Q_1	Q_3	Hazard ratio [95% CI]
Age	61	71	1.452 [1.298, 1.631]
Fitted $\log_2(\text{PSA} + 1)$ value	2.359	3.074	0.991 [0.894, 1.108]
Fitted $\log_2(\text{PSA} + 1)$ velocity	-0.086	0.307	2.466 [1.927, 2.992]

81 *Appendix A.5. Assumption of t-distributed (df=3) Error Terms*

82 With regards to the choice of the distribution for the error term ε for
83 the PSA measurements (see Equation 1), we attempted fitting multiple joint
84 models differing in error distribution, namely t-distribution with three, and
85 four degrees of freedom, and a normal distribution for the error term. How-
86 ever, the model assumption for the error term were best met by the model
87 with t-distribution having three degrees of freedom. The quantile-quantile
88 plot of subject-specific residuals for the corresponding model in Panel A of
89 Figure 3, shows that the assumption of t-distributed (df=3) errors is reason-
90 ably met by the fitted model.

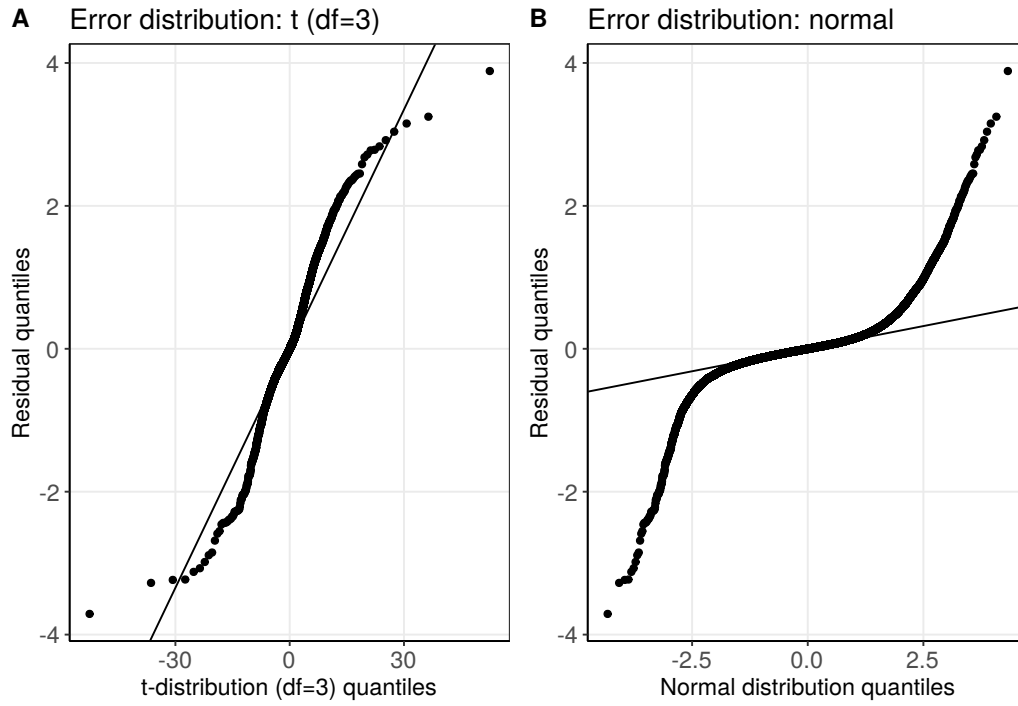


Figure 3: Quantile-quantile plot of subject-specific residuals from the joint models fitted to the PRIAS dataset. **Panel A:** model assuming a t-distribution ($df=3$) for the error term ε (see Equation 1). **Panel B:** model assuming a normal distribution for the error term ε .

91 Appendix B. Obtaining Dynamic Risk Predictions from the Joint 92 Model

Let us assume a new patient j , for whom we need to estimate the risk of GS7. Let his current follow-up visit time be s , latest time of biopsy be t , observed vector PSA measurements be $\mathcal{Y}_j(s)$. The combined information from the observed data about the time of GS7, is given by the following posterior predictive distribution $g(T_j^*)$ of his time T_j^* of GS7:

$$\begin{aligned} g(T_j^*) &= p\{T_j^* \mid T_j^* > t, \mathcal{Y}_j(s), \mathcal{D}_n\} \\ &= \int \int p(T_j^* \mid T_j^* > t, \mathbf{b}_j, \boldsymbol{\theta}) \\ &\quad \times p\{\mathbf{b}_j \mid T_j^* > t, \mathcal{Y}_j(s), \boldsymbol{\theta}\} p(\boldsymbol{\theta} \mid \mathcal{D}_n) d\mathbf{b}_j d\boldsymbol{\theta}. \end{aligned}$$

93 The distribution $g(T_j^*)$ depends not only depends on the observed data of the
94 patient $T_j^* > t, \mathcal{Y}_j(s)$, but also depends on the information from the PRIAS
95 dataset \mathcal{D}_n . To this the the posterior distribution of random effects \mathbf{b}_j and
96 posterior distribution of the vector of all parameters $\boldsymbol{\theta}$ are utilized, respec-
97 tively. The distribution $g(T_j^*)$ can be estimated as detailed in Rizopoulos
98 et al. [7]. Since, majority of the prostate cancer patients do not obtain GS7
99 in the ten year follow-up period of PRIAS, $g(T_j^*)$ can only be estimated for
100 time points falling within the ten year follow-up.

The cumulative risk of GS7 can be derived from $g(T_j^*)$ as given in [7]. It is given by:

$$R_j(u \mid t, s) = \Pr\{T_j^* > u \mid T_j^* > t, \mathcal{Y}_j(s), \mathcal{D}_n\}, \quad u \geq t. \quad (4)$$

101 The personalized risk profile of the patient (see Panel C, Figure 4) updates
102 as more data is gathered over follow-up visits.

103 Appendix B.1. Validation of Risk Predictions

104 We validated the predictions of GS7 internally within the PRIAS dataset,
105 as well as externally in five largest AS cohorts from the GAP3 database
106 [8]. These are the University of Toronto AS (Toronto), Johns Hopkins AS
107 (JHAS), Memorial Sloan Kettering Cancer Center AS (MSKCC), King's Col-
108 lege London AS (KCL), and Michigan Urological Surgery Improvement Col-
109 laborative AS (MUSIC). In all of these cohorts, we calculated the area under
110 the receiver operating characteristic curve or AUC [7] as a measure of dis-
111 crimination between patients who obtain GS7 and those do not obtain GS7.

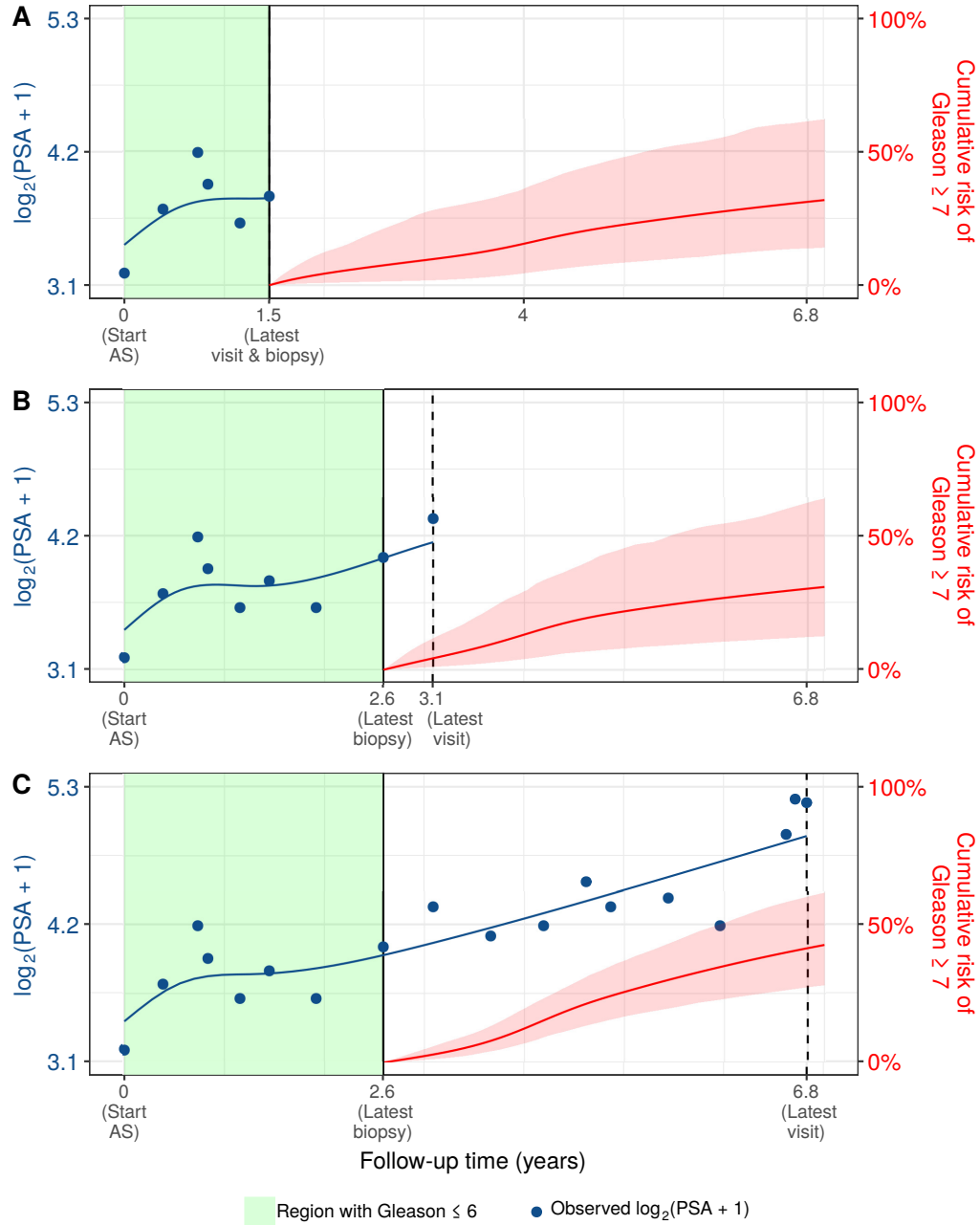


Figure 4: **Cumulative risk of Gleason ≥ 7 (GS7) changing dynamically over follow-up** as more patient data is gathered. The three **Panels A,B and C:** are ordered by the time of the latest visit (dashed vertical black line) of a new patient. At each of the latest follow-up visits, we combine the information from observed PSA measurements (shown in blue), and latest time of negative biopsy (solid vertical black line) to obtain the updated cumulative risk profile (shown in red) of the patient.

112 We also calculated root mean squared prediction error or RMSPE [7] as a
 113 measure of calibration. Both AUC and RMSPE take a value between 0 and
 114 1. Ideally RMSPE should be 0 and AUC should 1. In addition, it is preferred
 115 that $AUC > 0.5$ because an $AUC \leq 0.5$ indicates that the model performs
 116 worse than random discrimination. Since AS studies are longitudinal in na-
 117 ture, AUC and RMSPE are also time dependent. More specifically, given the
 118 time of latest biopsy t , and history of PSA measurements up to time s , we
 119 calculate AUC and RMSPE for a medically relevant time frame $(t, s]$, within
 120 which the occurrence of GS7 is of interest. In the case of prostate cancer,
 121 at any point in time s it is of interest to identify patients who may have ob-
 122 tained GS7 in the last one year $(s - 1, s]$. That is we set $t = s - 1$. We then
 123 calculate AUC and RMSPE at a gap of every six months (follow-up sched-
 124 ule of PRIAS) until year five (95-percentile of the observed times of GS7),
 125 that is, $se\{1, 1.5, \dots, 5\}$ years. The resulting estimates are summarized in
 126 Figure 5, and in Table 6 to Table 11.

Table 6: **Internal Validation of predictions of Gleason ≥ 7 (GS7) in PRIAS cohort.** The area under the receiver operating characteristic curve or AUC (measure of discrimination) root mean squared prediction error or RMSPE (measure of calibration) are calculated over the follow-up period at a gap of 6 months. In addition bootstrapped 95% confidence intervals (CI) are also presented.

Follow-up period (years)	AUC (95% CI)	RMSPE (95%CI)
0.0 to 1.0	0.656 [0.623, 0.690]	0.227 [0.223, 0.236]
0.5 to 1.5	0.657 [0.641, 0.671]	0.376 [0.371, 0.382]
1.0 to 2.0	0.663 [0.651, 0.678]	0.371 [0.364, 0.379]
1.5 to 2.5	0.650 [0.600, 0.684]	0.253 [0.245, 0.263]
2.0 to 3.0	0.676 [0.641, 0.725]	0.252 [0.241, 0.262]
2.5 to 3.5	0.689 [0.629, 0.732]	0.238 [0.224, 0.251]
3.0 to 4.0	0.652 [0.614, 0.709]	0.273 [0.263, 0.285]
3.5 to 4.5	0.625 [0.591, 0.663]	0.338 [0.326, 0.349]
4.0 to 5.0	0.623 [0.587, 0.657]	0.338 [0.325, 0.350]

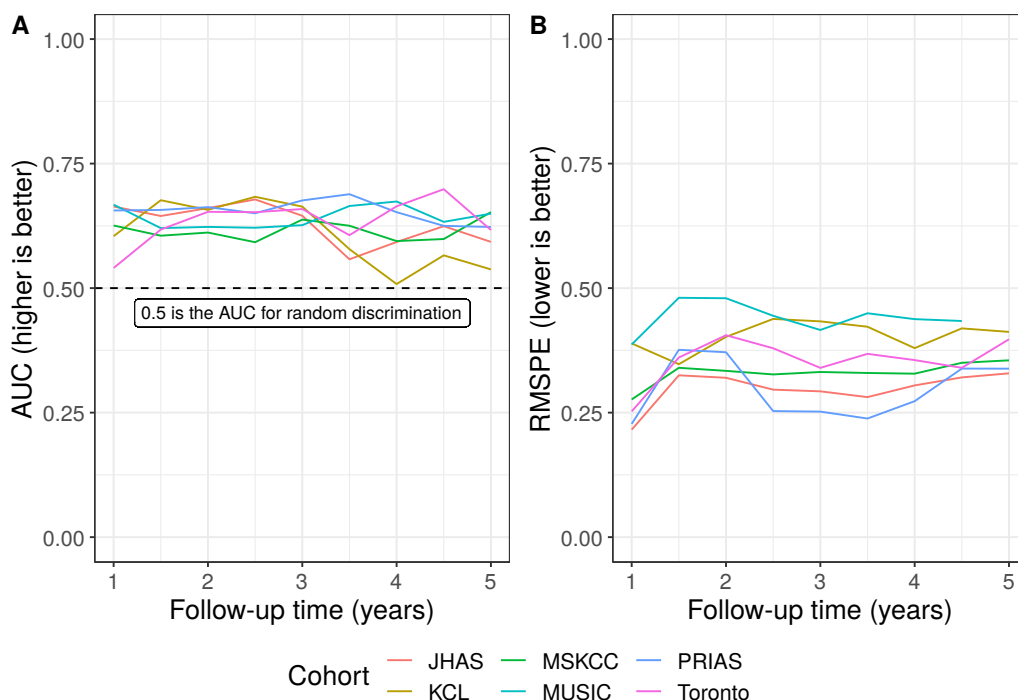


Figure 5: **Validation of predictions of Gleason ≥ 7 (GS7).** In **Panel A** we can see that the time dependent area under the receiver operating characteristic curve or AUC (measure of discrimination) is above 0.5 in PRIAS (internal validation), and Toronto, JHAS, MSKCC, KCL, and MUSIC AS cohorts (external validation). In **Panel B** we can see that the time dependent root mean squared prediction error or RMSPE (measure of calibration) is similar for PRIAS, and JHAS and Toronto cohorts. The bootstrapped 95% confidence interval for these estimates are presented in Table 6 to Table 10. Full names of Cohorts are *PRIAS*: Prostate Cancer International Active Surveillance, *Toronto*: University of Toronto Active Surveillance, *JHAS*: Johns Hopkins Active Surveillance, *MSKCC*: Memorial Sloan Kettering Cancer Center Active Surveillance, *KCL*: King's College London Active Surveillance, *MUSIC*: Michigan Urological Surgery Improvement Collaborative Active Surveillance.

Table 7: **External Validation of predictions of Gleason ≥ 7 (GS7) in University of Toronto Active Surveillance cohort.** The area under the receiver operating characteristic curve or AUC (measure of discrimination) root mean squared prediction error or RMSPE (measure of calibration) are calculated over the follow-up period at a gap of 6 months. In addition bootstrapped 95% confidence intervals (CI) are also presented.

Follow-up period (years)	AUC (95% CI)	RMSPE (95%CI)
0.0 to 1.0	0.540 [0.493, 0.595]	0.252 [0.236, 0.272]
0.5 to 1.5	0.618 [0.562, 0.660]	0.361 [0.350, 0.373]
1.0 to 2.0	0.653 [0.580, 0.719]	0.405 [0.384, 0.428]
1.5 to 2.5	0.652 [0.596, 0.727]	0.379 [0.358, 0.408]
2.0 to 3.0	0.659 [0.565, 0.743]	0.340 [0.303, 0.369]
2.5 to 3.5	0.606 [0.548, 0.676]	0.368 [0.340, 0.401]
3.0 to 4.0	0.664 [0.583, 0.736]	0.355 [0.324, 0.391]
3.5 to 4.5	0.699 [0.610, 0.773]	0.340 [0.310, 0.374]
4.0 to 5.0	0.617 [0.546, 0.705]	0.397 [0.355, 0.425]

Table 8: **External Validation of predictions of Gleason ≥ 7 (GS7) in Johns Hopkins Active Surveillance cohort.** The area under the receiver operating characteristic curve or AUC (measure of discrimination) root mean squared prediction error or RMSPE (measure of calibration) are calculated over the follow-up period at a gap of 6 months. In addition bootstrapped 95% confidence intervals (CI) are also presented.

Follow-up period (years)	AUC (95% CI)	RMSPE (95%CI)
0.0 to 1.0	0.664 [0.604, 0.743]	0.216 [0.198, 0.236]
0.5 to 1.5	0.645 [0.597, 0.695]	0.325 [0.310, 0.339]
1.0 to 2.0	0.661 [0.615, 0.707]	0.320 [0.300, 0.335]
1.5 to 2.5	0.678 [0.587, 0.736]	0.296 [0.277, 0.312]
2.0 to 3.0	0.645 [0.595, 0.701]	0.293 [0.268, 0.317]
2.5 to 3.5	0.558 [0.445, 0.622]	0.281 [0.256, 0.307]
3.0 to 4.0	0.593 [0.498, 0.693]	0.305 [0.281, 0.329]
3.5 to 4.5	0.624 [0.527, 0.690]	0.321 [0.294, 0.340]
4.0 to 5.0	0.593 [0.483, 0.694]	0.329 [0.306, 0.352]

Table 9: **External Validation of predictions of Gleason ≥ 7 (GS7) in Memorial Sloan Kettering Cancer Center Active Surveillance cohort.** The area under the receiver operating characteristic curve or AUC (measure of discrimination) root mean squared prediction error or RMSPE (measure of calibration) are calculated over the follow-up period at a gap of 6 months. In addition bootstrapped 95% confidence intervals (CI) are also presented.

Follow-up period (years)	AUC (95% CI)	RMSPE (95%CI)
0.0 to 1.0	0.626 [0.558, 0.681]	0.276 [0.260, 0.297]
0.5 to 1.5	0.605 [0.539, 0.666]	0.340 [0.321, 0.360]
1.0 to 2.0	0.612 [0.564, 0.672]	0.334 [0.316, 0.350]
1.5 to 2.5	0.592 [0.502, 0.670]	0.327 [0.306, 0.345]
2.0 to 3.0	0.638 [0.548, 0.720]	0.332 [0.304, 0.363]
2.5 to 3.5	0.625 [0.542, 0.717]	0.330 [0.303, 0.371]
3.0 to 4.0	0.594 [0.511, 0.655]	0.328 [0.281, 0.368]
3.5 to 4.5	0.599 [0.481, 0.740]	0.350 [0.312, 0.373]
4.0 to 5.0	0.653 [0.562, 0.724]	0.355 [0.320, 0.380]

Table 10: **External Validation of predictions of Gleason ≥ 7 (GS7) in King's College London Active Surveillance cohort.** The area under the receiver operating characteristic curve or AUC (measure of discrimination) root mean squared prediction error or RMSPE (measure of calibration) are calculated over the follow-up period at a gap of 6 months. In addition bootstrapped 95% confidence intervals (CI) are also presented.

Follow-up period (years)	AUC (95% CI)	RMSPE (95%CI)
0.0 to 1.0	0.604 [0.548, 0.663]	0.389 [0.366, 0.411]
0.5 to 1.5	0.676 [0.603, 0.744]	0.347 [0.328, 0.372]
1.0 to 2.0	0.657 [0.578, 0.728]	0.402 [0.368, 0.426]
1.5 to 2.5	0.683 [0.595, 0.773]	0.438 [0.395, 0.469]
2.0 to 3.0	0.664 [0.576, 0.735]	0.433 [0.396, 0.467]
2.5 to 3.5	0.578 [0.443, 0.712]	0.422 [0.345, 0.479]
3.0 to 4.0	0.508 [0.358, 0.670]	0.380 [0.313, 0.452]
3.5 to 4.5	0.566 [0.346, 0.776]	0.419 [0.354, 0.484]
4.0 to 5.0	0.538 [0.295, 0.759]	0.412 [0.345, 0.470]

Table 11: **External Validation of predictions of Gleason ≥ 7 (GS7) in Michigan Urological Surgery Improvement Collaborative Active Surveillance cohort.** The area under the receiver operating characteristic curve or AUC (measure of discrimination) root mean squared prediction error or RMSPE (measure of calibration) are calculated over the follow-up period at a gap of 6 months. In addition bootstrapped 95% confidence intervals (CI) are also presented.

Follow-up period (years)	AUC (95% CI)	RMSPE (95%CI)
0.0 to 1.0	0.667 [0.616, 0.703]	0.387 [0.369, 0.409]
0.5 to 1.5	0.620 [0.566, 0.646]	0.481 [0.462, 0.495]
1.0 to 2.0	0.623 [0.569, 0.666]	0.480 [0.459, 0.501]
1.5 to 2.5	0.621 [0.580, 0.677]	0.444 [0.418, 0.472]
2.0 to 3.0	0.626 [0.464, 0.710]	0.416 [0.376, 0.459]
2.5 to 3.5	0.665 [0.554, 0.796]	0.449 [0.390, 0.493]
3.0 to 4.0	0.674 [0.540, 0.757]	0.438 [0.374, 0.483]
3.5 to 4.5	0.633 [0.410, 0.865]	0.434 [0.346, 0.485]
4.0 to 5.0	0.650 [0.248, 0.946]	– [–, –]

127 Appendix C. Personalized Biopsies Based on Risk of GS7

128 Consider some real patients from the PRIAS database shown in Figure 6
 129 to Figure 9. We intend to develop personalized schedule of biopsies for these
 130 patients. Using the joint model fitted to the PRIAS dataset, we first obtain
 131 their cumulative risk of GS7 over the entire follow-up period (see Equation 4).
 132 This cumulative risk accounts for their entire history of PSA as well as the
 133 time of their latest negative biopsy. For a new patient j we suggest a per-
 134 sonalized risk based biopsy at time s if their cumulative risk of GS7 denoted
 135 by $R_j(s | t, s)$ at s , given the time of their latest negative biopsy t , is above
 136 a certain threshold (e.g., 10% risk). Suppose that in this way a decision of
 137 biopsy is taken at time s . Since patients may be removed from AS upon
 138 detection of GS7, schedule of future biopsies is made by assuming that GS7
 139 is not detected at time s . Thus, for a decision of biopsy at the next visit time
 140 $s + 1$, the cumulative risk of GS7 denoted by $R_j(s + 1 | s, s)$ that the time of
 141 latest negative biopsy is s . Similarly, if $R_j(s + 1 | s, s) < 10\%$, then we decide
 142 for a biopsy at a subsequent time $s + 2$ using the threshold $R_j(s + 2 | s, s)$.
 143 On the other hand if $R_j(s + 1 | s, s) \geq 10\%$ then then we decide for a biopsy
 144 at time $s + 2$ using the threshold $R_j(s + 2 | s + 1, s)$. While scheduling
 145 these biopsies we always maintain a minimum gap of one year. Personalized
 146 schedules can also be made with any other risk threshold such as 5% or 15%.

To assist patients in making an informed choice for a schedule, be it per-
 sonalized or fixed, we provide them patient-specific consequences of following
 each schedule. To this end, we first calculate the probability of occurrence of
 GS7 between successive biopsies of each schedule. Using these probabilities
 we then obtain the expected delay in detection of GS7 for following that
 schedule. Thus, patients have a method to compare across various schedules
 in terms of the personalized burden (time and total biopsies), and personal-
 ized benefit (less delay in detection of GS7 is beneficial). Suppose once again
 that for patient j , the time of latest negative biopsy is t , and current visit
 time is $s > t$. Then equation for the expected delay $D_j(\mathcal{S} | t, s)$ in detection
 of GS7 using schedule of biopsies $\mathcal{S} = \{t_1, \dots, t_h\}$, where $t_1 \geq s$, and t_h is
 the horizon time up to which we want to schedule biopsies, is given by:

$$\begin{aligned}
 D_j(\mathcal{S} | t, s) = & \sum_{v=1}^{h-1} \left\{ R_j(t_{v+1} | t, s) - R_j(t_v | t, s) \right\} \\
 & \times \left\{ t_{v+1} - t_v - \int_{t_v}^{t_{v+1}} \frac{R_j(t_{v+1} | t, s) - R_j(u | t, s)}{R_j(t_{v+1} | t, s) - R_j(t_v | t, s)} du \right\}
 \end{aligned} \tag{5}$$

147 The personalized and fixed schedules, and their consequences for a few real
148 patients from the PRIAS dataset are shown in Figure 6 to Figure 9. For all
149 patients, the risk estimates are smaller after a negative biopsy.

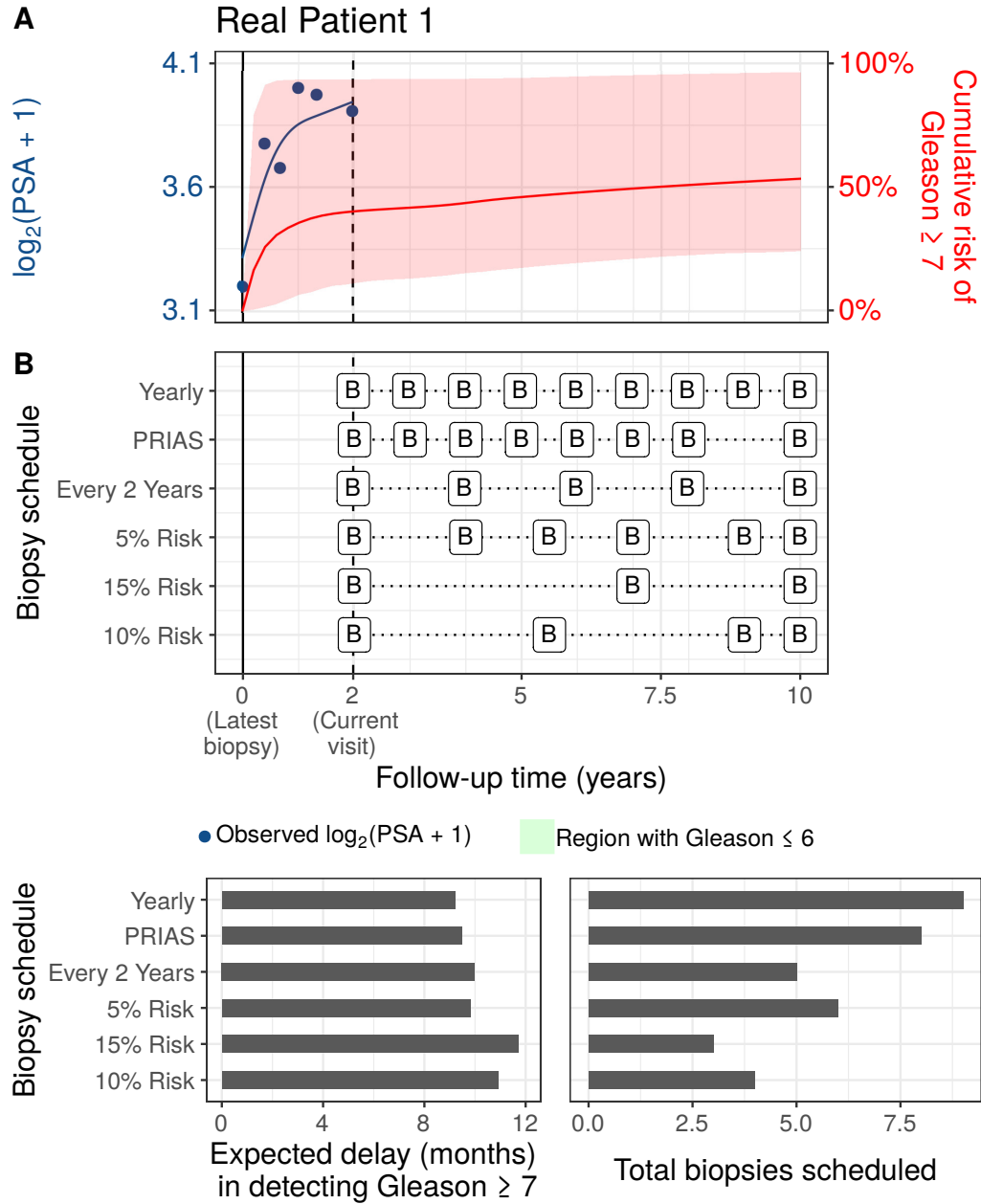


Figure 6: **Personalized and fixed schedules of biopsies patient 1.** **Panel A:** shows the observed and fitted $\log_2(\text{PSA} + 1)$ measurements (Equation 1), and the dynamic cumulative risk of Gleason ≥ 7 (see Appendix B) over follow-up period. **Panel B** shows the personalized and fixed schedules of biopsies with a 'B' indicating times of biopsies. In the bottom two panels, the various schedules are compared in terms of the number of biopsies they schedule, and the expected delay in detection of Gleason ≥ 7 if they are followed.

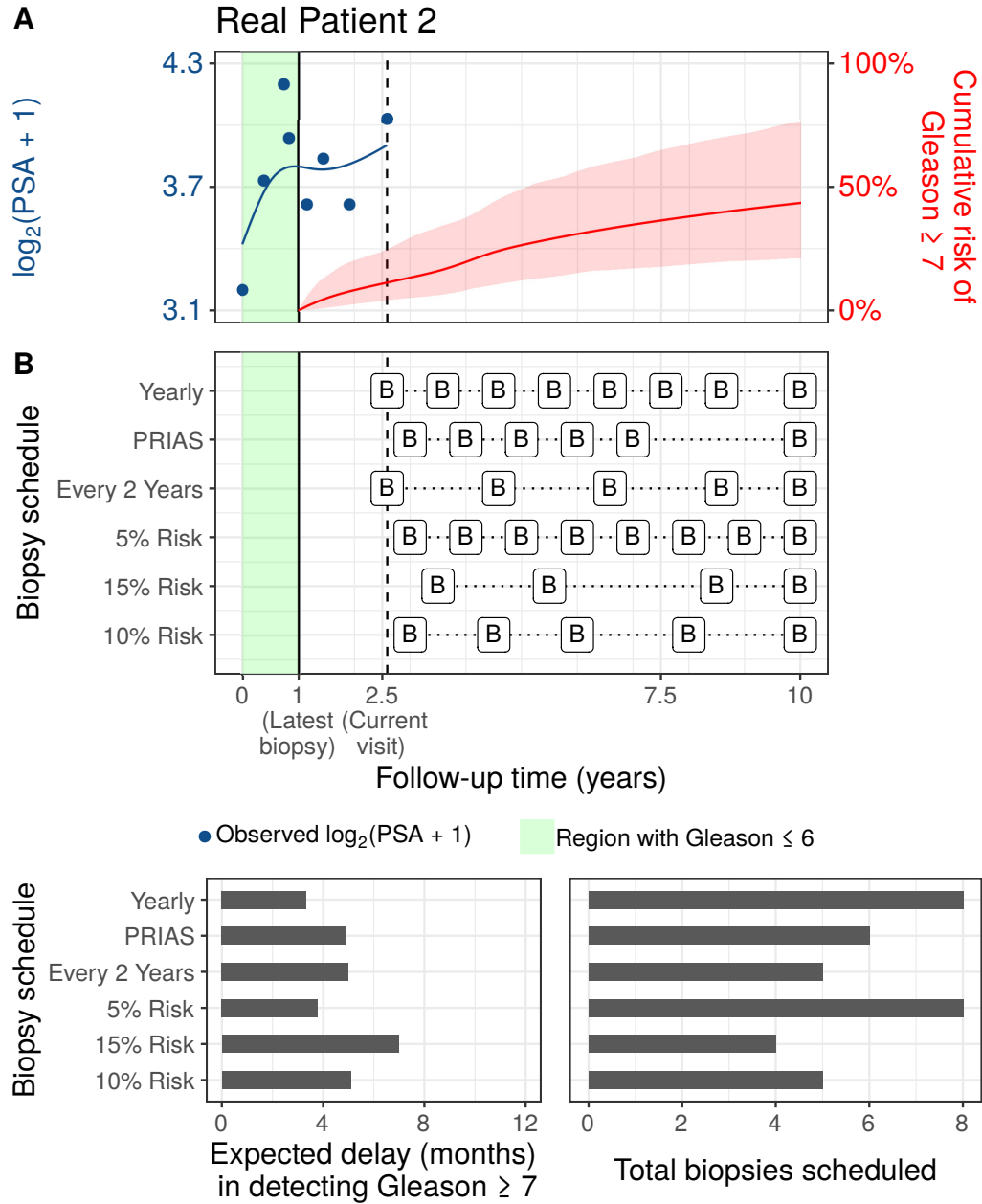


Figure 7: **Personalized and fixed schedules of biopsies patient 2.** **Panel A:** shows the observed and fitted $\log_2(\text{PSA} + 1)$ measurements (Equation 1), and the dynamic cumulative risk of Gleason ≥ 7 (see Appendix B) over follow-up period. **Panel B** shows the personalized and fixed schedules of biopsies with a ‘B’ indicating times of biopsies. In the bottom two panels, the various schedules are compared in terms of the number of biopsies they schedule, and the expected delay in detection of Gleason ≥ 7 if they are followed.

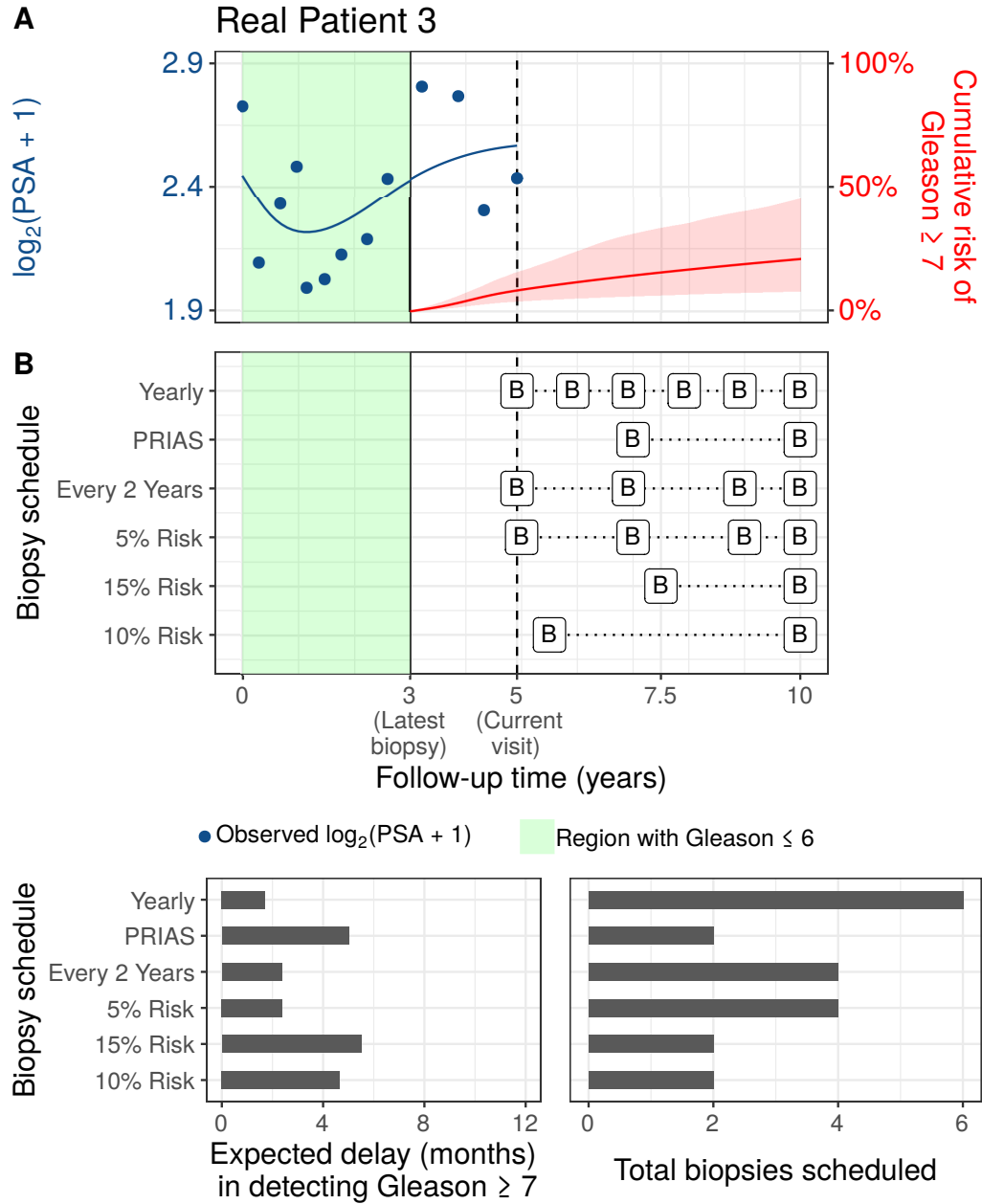


Figure 8: **Personalized and fixed schedules of biopsies patient 3.** **Panel A:** shows the observed and fitted $\log_2(\text{PSA} + 1)$ measurements (Equation 1), and the dynamic cumulative risk of Gleason ≥ 7 (see Appendix B) over follow-up period. **Panel B** shows the personalized and fixed schedules of biopsies with a 'B' indicating times of biopsies. In the bottom two panels, the various schedules are compared in terms of the number of biopsies they schedule, and the expected delay in detection of Gleason ≥ 7 if they are followed.

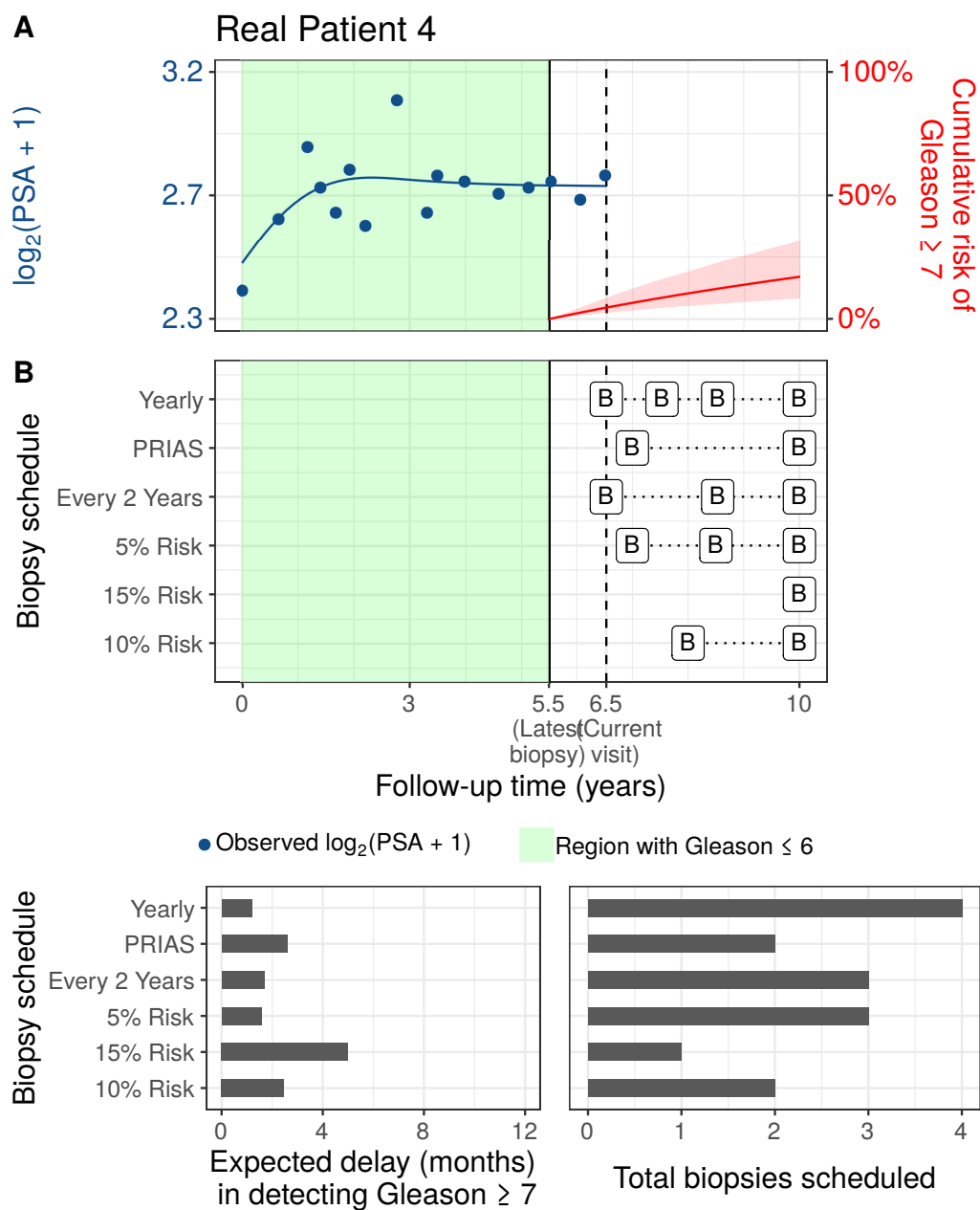


Figure 9: **Personalized and fixed schedules of biopsies patient 4.** **Panel A:** shows the observed and fitted $\log_2(\text{PSA} + 1)$ measurements (Equation 1), and the dynamic cumulative risk of Gleason ≥ 7 (see Appendix B) over follow-up period. **Panel B** shows the personalized and fixed schedules of biopsies with a 'B' indicating times of biopsies. In the bottom two panels, the various schedules are compared in terms of the number of biopsies they schedule, and the expected delay in detection of Gleason ≥ 7 if they are followed.

150 **Appendix D. Web Application for Practical Use of Personalized**
151 **Schedule of Biopsies**

152 Appendix E. Source Code

153 The R code for fitting the joint model to the PRIAS dataset, is at https://github.com/anirudhtomer/prias/tree/master/src/clinical_gap3. We
 154 refer to this location as ‘R_HOME’ in the rest of this document.
 155

156 *Appendix E.1. Fitting the Joint Model to the PRIAS dataset*

157 **Accessing the dataset:** The PRIAS dataset is not openly accessible.
 158 However, access to the database can be requested via the contact links at
 159 www.prias-project.org.
 160

161 **Formatting the dataset:** This dataset however is in the so-called
 162 wide format and also requires removal of incorrect entries. This can be
 163 done via the R script `R_HOME/dataset_cleaning.R`. This will lead to two
 164 R objects, namely ‘`prias_final.id`’ and ‘`prias_long_final`’. The ‘`prias_final.id`’
 165 object contains information about time of GS7 for PRIAS patients. The
 166 ‘`prias_long_final`’ object contains longitudinal PSA measurements, the time
 167 of biopsies and results of biopsies.
 168

169 **Fitting the joint model:** We use a joint model for time to event
 170 and longitudinal data to model the evolution of PSA measurements over
 171 time, and to simultaneously model their association with the risk of GS7.
 172 The R package we use for this purpose is called **JMbayes** (<https://cran.r-project.org/web/packages/JMbayes/JMbayes.pdf>). The API we use, how-
 173 ever, are currently not hosted on CRAN, and can be found here: <https://github.com/anirudhtomer/JMbayes>. The joint model can be fitted via
 174 the script `R_HOME/analysis.R`. It takes roughly 6 hours to run on an Intel
 175 core-i5 machine with 4 cores, and 8GB of RAM.
 176

177 The graphs presented in the main manuscript, and the supplementary
 178 material can be generated by the scripts in `R_HOME/plots/`.
 179

180 *Appendix E.2. Validation of Predictions of GS7*

181 Validations can be done using the script `R_HOME/auc_brier/auc_prederr_`
 182 `no_dre.R`. For external validation access to GAP3 database is required.

183 *Appendix E.3. Creating Personalized Schedules of Biopsies*

184 Once a joint model is fitted to the PRIAS dataset, personalized schedules
 185 of biopsies based on risk of GS7 for new patients can be developed using the

186 script `R_HOME/compareSchedules.R`. This script also provides fixed biopsy
187 schedules for the patients. In addition with each schedule, the expected delay
188 in detection of GS7 is also provided.

189 *Appendix E.4. Source Code for Web Application*

190 Source for the shiny web application which provides biopsy schedules for
191 patients can be found at `R_HOME/shinyapp`

192 References

- 193 1. Bul M, Zhu X, Valdagni R, Pickles T, Kakehi Y, Rannikko A, Bjartell
194 A, Van Der Schoot DK, Cornel EB, Conti GN, et al. Active surveillance
195 for low-risk prostate cancer worldwide: the prias study. *European urology*
196 2013;63(4):597–603.
- 197 2. Pearson JD, Morrell CH, Landis PK, Carter HB, Brant LJ. Mixed-effects
198 regression models for studying the natural history of prostate disease.
199 *Statistics in Medicine* 1994;13(5-7):587–601.
- 200 3. Lin H, McCulloch CE, Turnbull BW, Slate EH, Clark LC. A latent
201 class mixed model for analysing biomarker trajectories with irregularly
202 scheduled observations. *Statistics in Medicine* 2000;19(10):1303–18.
- 203 4. De Boor C. A practical guide to splines; vol. 27. Springer-Verlag New
204 York; 1978.
- 205 5. Eilers PH, Marx BD. Flexible smoothing with B-splines and penalties.
206 *Statistical Science* 1996;11(2):89–121.
- 207 6. Rizopoulos D. The R package JMBayes for fitting joint models for lon-
208 gitudinal and time-to-event data using MCMC. *Journal of Statistical*
209 *Software* 2016;72(7):1–46.
- 210 7. Rizopoulos D, Molenberghs G, Lesaffre EM. Dynamic predictions with
211 time-dependent covariates in survival analysis using joint modeling and
212 landmarking. *Biometrical Journal* 2017;59(6):1261–76.
- 213 8. Bruinsma SM, Zhang L, Roobol MJ, Bangma CH, Steyerberg EW,
214 Nieboer D, Van Hemelrijck M, consortium MFGAPPCASG, Trock B,
215 Ehdaie B, et al. The movember foundation’s gap3 cohort: a profile of the
216 largest global prostate cancer active surveillance database to date. *BJU*
217 *international* 2018;121(5):737–44.